RAFAL: RANDOM FACED ACOUSTIC LENS USED TO MODEL INTERNAL WAVES EFFECTS ON UNDERWATER ACOUSTIC PROPAGATION

Gaultier Real, Xavier Cristol, Dominique Habault, Jean-Pierre Sessarego, Dominique Fattaccioli

RAFAL: *RA*NDOM *F*ACED *A*COUSTIC *L*ENS USED TO MODEL INTERNAL WAVES EFFECTS ON UNDERWATER ACOUSTIC PROPAGATION.

Gaultier Real[a,b], Xavier Cristol[b], Dominique Habault[a], Jean-Pierre Sessarego[a], and Dominique Fattaccioli[c]

[a]: Laboratoire de Mécanique et d'Acoustique (LMA), CNRS, 31 Chemin Joseph Aiguier, 13402 Marseille cedex 20, France, mail : real@lma.cnrs-mrs.fr, habault@lma.cnrs-mrs.fr, sessarego@lma.cnrs-mrs.fr.
[b]: Thales Underwater Systems SAS, 525 route des Dolines, 06903 Sophia-Antipolis, France, mail : xavier.cristol@fr.thalesgroup.com.
[c]: DGA Naval Systems, avenue de la Tour Royale, BP 40915, 83050 Toulon Cedex, France, mail : dominique.fattaccioli@intradef.gouv.fr.

Abstract: *We present here an experimental protocol to reproduce the effects of linear internal waves (LIW) on acoustic wave propagation in a very controlled and reproducible manner. In fact, the experiment consists in propagating an ultrasonic wave through an acoustic lens presenting a plane input face and a randomly rough output face. The so-called RAFAL (Random Faced Acoustic Lens) was designed so that the roughness of the output face induce resulting acoustic pressure field featuring typical characteristics of propagation though LIW.To ensure representativeness of our model, we conducted analytical calculations leading to dimensionless parameters equivalent to the ones developed by Flatté (strength parameter Φ and diffraction parameter Λ). In our case, the strength parameter was calculated after evaluation of the phase of the average acoustic field propagated through the RAFALS, whereas our diffraction parameter was evaluated using the phase sensitivity kernel. On the other hand, we calculated the ratio of correlation length of the acoustic field to wavelength. Measurements were conducted on several RAFALS, corresponding to various realistic configurations. The regimes of saturation (full and partial) and unsaturation were explored. The results are presented in terms of order 2 (coherence function) and order 4 (intensity) statistics and demonstrate the accuracy of our experimental scheme with respect to real scale simulations and simplified theory. Other representations, such as phasors, also show a very meaningful behavior.*

Keywords: *coherence, tank experiment, acoustic fluctuations, internal waves.*

1. INTRODUCTION.

This paper addresses the topic of acoustic wave distortions when they travel through an ocean subject to linear internal waves (LIW). Transverse to many scientific fields [1-3], the phenomena associated with this topic are of great influence on the system performance (detection, localization) [4-7]. A novel experimental protocol is proposed here: it allows to isolate the fluctuations due to LIW from other sources of signal de-coherence (scattering from the sea surface or the seabed) and provide reproducibility and control. Our scheme differs from what can be found in the literature [8-10] since we propagate a signal through a Random Faced Acoustic Lens (or RAFAL), whose characteristics are given in the present paper. The relevance of our scheme is demonstrated using a statistical study (second and fourth order moments of the received acoustic pressure).

2. EXPERIMENTAL PROTOCOL.

The experiments conducted here follow the scheme described in reference [11]. An ultrasonic signal (f=2.25MHz) is propagated through the RAFAL (manufactured as presented in reference [11]), and the measurement of the acoustic pressure field throughout specific regions of the three-dimensional space is conducted. A diagram of the experimental configuration is given in Fig.2:

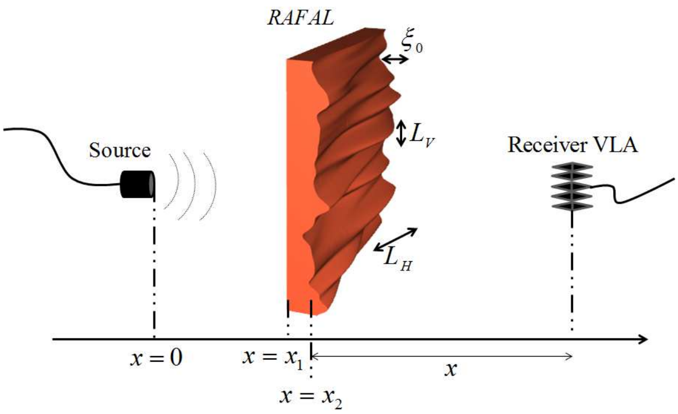

Fig.2: Experimental configuration diagram.

3. CONFIGURATIONS STUDIED

3.1 CORRESPONDANCE WITH OCEANIC CONFIGURATIONS.

To ensure the representativeness of our experiment, the dimensionless parameters defined by Flatté in [12] are used. Because they both depend on environmental parameters (correlation length and amplitude of the sound speed fluctuations), they are not adapted to our experimental configuration. In reference [11], statistics of rays were used to obtain Λ and Φ in our case. A more robust method is proposed here: Φ is obtained from the averaged acoustic field (from 2D Fourier transforms based analytical calculations), and Λ is calculated using the Fréchet derivative of the acoustic field, leading to the evaluation of the Fresnel radius (linked to the phase sensitivity kernel [13,14]). The expressions obtained for the scaled dimensionless parameters, denoted Λ_S and Φ_S , are:

$$\Lambda_S = \frac{R_F^2}{2\pi L_V^2}, \tag{1}$$

$$\Phi_S = k\xi_0\left(1-\frac{c_1}{c_2}\right), \tag{2}$$

where k is the wavenumber in water, ξ_0 is the standard deviation of the RAFAL's output face amplitude, c_1 is the sound speed in water and c_2 is the sound speed in the RAFAL.We also define two others dimensionless parameters: the ratio of the acoustic field correlation length to the wavelength (in both vertical and horizontal directions). In an oceanic environment, these parameters are obtained using Tatarskii's work [3]. Here, they derive from calculation of the intercorrelation of the analytically calculated acoustic field:

$$\frac{L_Z}{\lambda} = \frac{1}{2\pi}\frac{L_V}{\xi_0}\frac{1}{1-\frac{c_1}{c_2}}\left(1+\frac{x}{x_1+\frac{c_2}{c_1}\left(x_2-x_1\right)}\right), \tag{3}$$

$$\frac{L_Y}{\lambda} = \frac{1}{2\pi}\frac{L_H}{\xi_0}\frac{1}{1-\frac{c_1}{c_2}}\left(1+\frac{x}{x_1+\frac{c_2}{c_1}\left(x_2-x_1\right)}\right), \tag{4}$$

Overall, the scaled experiment configurations studied and their correspondence in an oceanic medium are given in Figure 3:

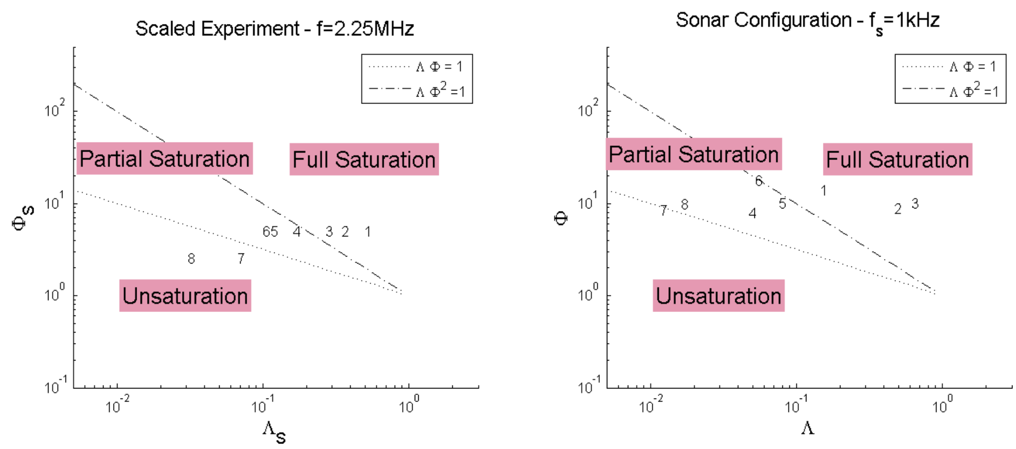

Fig.3: Λ-Φ plane.

4. EXPERIMENTAL RESULTS.

4.1 RADIUS OF COHERENCE.

The mutual coherence function (MCF) is often used to evaluate the correlation of the acoustic wave received by a linear array. The interspectral matrix is first computed, then averaged across the iso-spaced sensors, leading to a function of the sensor spacing $\Gamma(l)$, such that [5,15]:

$$\Gamma(l)=\left|\left\langle\left\langle\frac{p(n)\,p^*(n+l)}{|p(n)||p(n+l)|}\right\rangle_N\right\rangle_{N_r}\right|. \qquad (5)$$

In Figure 4, the radius of coherence (sensor spacing ρ_c for which $\Gamma(\rho_c)=\exp(-0.5)$ [16]) is displayed for the configurations explored in this series of experiments (see Figure 3). The calculation is performed using the measurements (red circles), simulations of the RAFAL experiment (magenta diamonds), simulations in the corresponding oceanic environment [17] (cyan squares) and simplified theory [18] (blue crosses).

A good agreement is found in most configurations (except FS1 and PS1), since the value and evolution of the radius of coherence is consistent throughout the explored configurations. We may explain the higher differences in ρ_c in the case of configurations FS1 and PS1 because of the experimental parameter that they have in common: the distance between the source and the receiving VLA was the highest in these configurations. The propagation and diffraction of the acoustic wave may have overcompensated the effects of the presence of the RAFAL. This phenomenon is not observed in the case of P3DCOM because the perturbation, in the ocean, is not local but continuous.

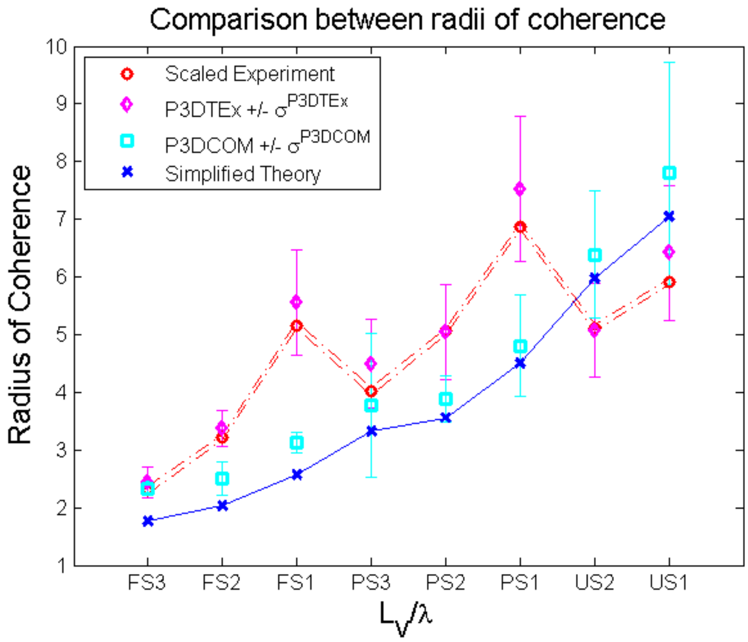

Fig.4: ρ_c *estimation.*

4.2 COMPLEX PRESSURE DISTRIBUTION.

The real and imaginary parts of the complex pressure are displayed for each realization of the medium. The distribution of the complex pressure is compared to the mean pressure distribution ($p_0 = \sqrt{\left\langle |p|^2 \right\rangle_{N_r}}$, displayed with the dashed line). The CPDs exhibited in the regimes of fluctuations show characteristic behaviours [19]: in the fully saturated regime, important phase variations are noticed, inducing a chaotic representation of the so-called phasor. In the regime of unsaturation, the CPD is supposed to follow the circle of mean complex pressure. A transition between these is found in the partial saturation case, with a more uniform CPD. Figure 5 depicts the CPD for three configurations (FS3, PS1 and US1, from left to right) in three different environments: the first line displays the CPD corresponding to the experimental data, the second line displays the same quantity calculated using P3DTEx, with ten times more realizations than the experimental data ; finally, the third line displays the CPD calculated using P3DCOM, again, with ten times more realizations than the experimental data.

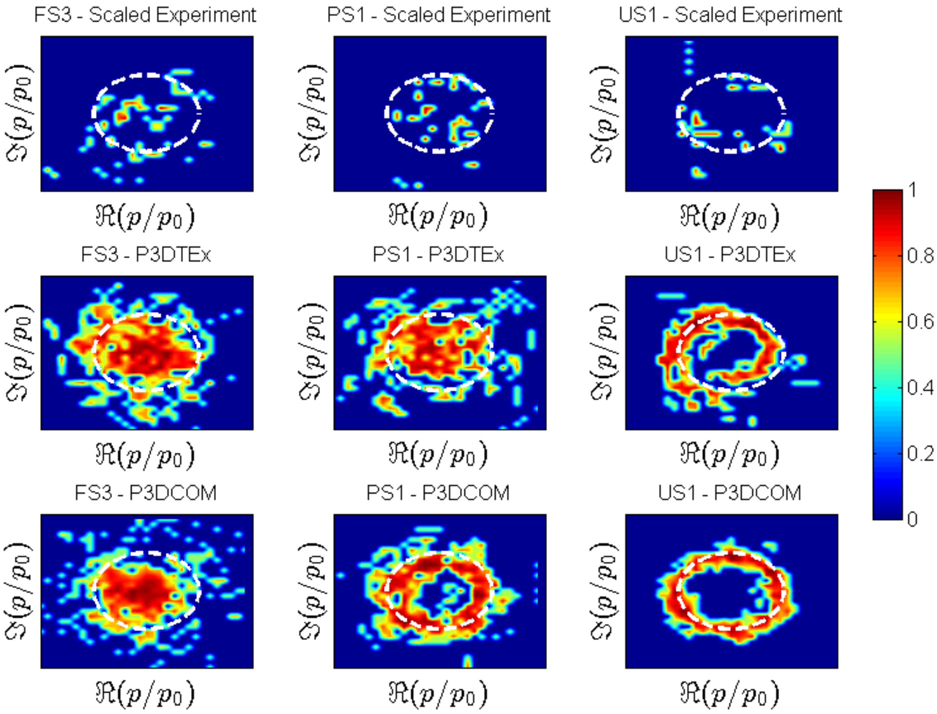

Fig.5: Complex pressure distribution.

4.3 INTENSITY DISTRIBUTION.

In this section, the higher order moment (4th order) is studied: the acoustic intensity I. More precisely, the distribution of the normalized intensity $I/\langle I \rangle$ is computed in three typical configurations (FS3, PS1 and US1, similarly as in section 4.2) for the experimental data and the simulations (P3DTEx and P3DCOM). The results, displayed in Figure 6, clearly show the relevance of our experimental scheme. In fact, the intensity distribution $W\left(I/\langle I \rangle\right)$ follows an exponential curve in the fully saturated case, and a log-normal distribution in the unsaturated case in all cases, despite the fact that the experimental data display far less realizations than the simulations. This results echoes the analysis in reference [10].
The partially saturated case is, once again, a transition between the two other cases.

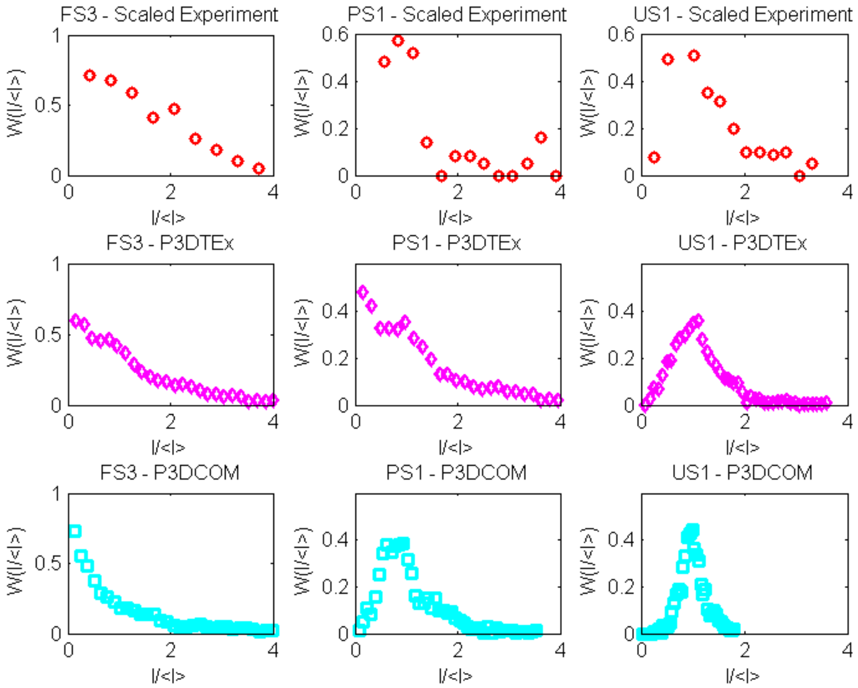

Fig.6: Intensity distribution.

5. CONCLUSION

We developed a highly reproducible experimental protocol in a controlled environment. The use of RAFAL to reproduce LIW effects on underwater acoustic propagation was proven to be relevant, since statistical tools such as the radius of coherence, the complex pressure distribution and the normalized intensity distribution displayed behaviours representative of oceanic configurations. The ability to acquire experimental data perturbed in a very controlled fashion is therefore provided here. It can be used to measure the influence of the type of medium fluctuations studied here on signal processing techniques.

ACKNOWLEDGMENT

This work is sponsored by a research grant of the Mission pour la Recherche et l'Innovation Scientifique (DGA – MRIS), the Laboratory of Mechanics and Acoustics (LMA – CNRS) and Thales Underwater Systems.

REFERENCES

[1] I. Newton, Opticks, (reprinted by Bell & Sons, London, 1931), p.107-111

[2] A. Ishimaru. *Wave propagation and scattering in random media, volume 2*, (Academic

press, New York, 1978), pp. 346-375.
[3] V.I. Tatarskii, *The Effects of the Turbulent Atmosphere on Wave Propagation*, (National Technical Information Servie, Springfield, VA, 1971), pp. 1-472.York, 2002), pp. 1-259.
[4] D. K. Wilson, “Performance bounds for acoustic direction-of-arrival arrays operating in atmospheric turbulence,” J. Acoust. Soc. Am. 103(3), 1306-1319 (1998).
[5] E.Y. Gorodetskaya, A.I. Malekhanov, A.G. Sazontov, and N.K. Vdovicheva, “Deep-water acoustic coherence at long ranges: Theoretical prediction and effects on large-array signal processing,” IEEE J. Ocean. Eng. 24(2), 156-171 (1999)
[6] D. Fattaccioli, X. Cristol, G. Picard Destelan, and P. Danet, “Sonar processing performance in random environments,” Proc. Of Underwater Acoustic Measurements (UAM 09), 21-26 June 2009, Nafplion, Greece, pp. 1-6.
[7] R. Laval and Y. Labasque, “Medium inhomogeneities and instabilities: Effects on spatial and temporal processing”, Proc. of the NATO Advanced Study Institute, 18-29 August 1980, Copenhagen, Denmark, pp. 41-70.
[8] P.F. Dobbins, Degradation of Coherence of Acoustic Signals Resulting from Inhomogeneities in the Sea, (Ph.D. dissertation, University of Bath (UK), 1989).
[9] N.P. Chotiros and B.V. Smith, “Sound amplitude fluctuations due to a temperature microstructure,” J. of Sound and Vibration 64(3), 349-369 (1979).
[10] P. Blanc-Benon and D. Juvé, “Intensity fluctuations of spherical acoustic waves propagating through thermal turbulence,” Waves in random media 3(2), 71-83 (1993).
[11] G. Real, J.-P. Sessarego, X. Cristol and D. Fattaccioli, “De-coherence effects in underwater acoustics: scaled experiments”, Proc. of the 2nd Underwater Acoustic Conference, 22-27 June 2014, Rhodes, Greece, pp. 1-8.
[12] R. Dashen, S.M. Flatt´e, W.H. Munk, K.M. Watson, and F. Zachariasen, *Sound transmission through a fluctuating ocean* (Cambridge University Press, London, 1979), pp. 1-299.
[13] E.K. Skarsoulis and B.D. Cornuelle, “Travel-time sensitivity kernels in ocean acoustic tomography,” J. Acoust. Soc. Am. 116(1), 227-238 (2004).
[14] H. Marquering, F.A. Dahlen, and G. Nolet, “Three-dimensional sensitivity kernels for finite-frequency traveltimes: the banana-doughnut paradox,” Geophysical J. Int. 137(3), 805-815 (1999).
[15] J.M. Collis, T.F. Duda, J.F. Lynch, and H.A. DeFerrari, “Observed limiting cases of horizontal field coherence and array performance in a time-varying internal wavefield,” J. Acoust. Soc. Am. 124(3), EL97-EL103 (2008).
[16] W.M. Carey, “The determination of signal coherence length based on signal coherence and gain measurements in deep and shallow water,” J. Acoust. Soc. Am. 104(2), 831-837 (1998).
[17] G. Real, X. Cristol, J.-P. Sessarego and D. Fattaccioli, “Propagation of acoustic waves through a spatially fluctuating medium: theoretical study of the physical phenomena Proc. of the 2nd Underwater Acoustic Conference, 22-27 June 2014, Rhodes, Greece, pp. 1-6.
[18] R. Dashen, S.M. Flatté, and S.A. Reynolds, “Path-integral treatment of acoustic mutual coherence functions for rays in a sound channel,” J. Acoust. Soc. Am. 77(5), 1716-1722 (1985).
[19] S. Flatté, “Wave propagation through random media: Contributions from ocean acoustics”, Proc. of IEEE, 1983, pp. 1267-1294.